S_1-S_0 Electronic Spectroscopy and ab Initio Calculations of *cis*-2-Methoxynaphthalene

T. Troxler

Departement für Chemie und Biochemie, Universität Bern, Freiestrasse 3, CH-3000 Bern 9, Switzerland

Received: December 10, 1997; In Final Form: April 1, 1998

The vibronic structure of the $S_1 \leftrightarrow S_0$ electronic transition of jet-cooled *cis*-2-methoxynaphthalene (2MXN) has been investigated in detail by use of laser-induced excitation and emission spectroscopy. Fluorescence hole-burning experiments were employed to establish vibronic excitations due to the presence of the *cis* isomer. Eighteen ground state and 15 excited state vibrational frequencies were assigned by analyses of 25 single vibronic level fluorescence (SVLF) spectra, including the methoxy and methyl torsional mode frequencies. Strong vibrational state mixing in S_1 was observed in several SVLF spectra at low vibrational excess energies, attributed to the combined appearance of Fermi resonances and Duschinsky rotation. Vibrational assignments of S_0 frequencies were supported by ab initio calculations, employing the RHF/6-31G** method. Optimization of ground state geometries revealed that the *cis* isomer is the lowest energetic ground state conformer of 2MXN, in agreement with experiment. Furthermore, excited state ab initio calculations using the CIS/6-31G** method predicted that the first excited state of *cis*-2MXN correlates with the S_2 state of parent naphthalene, exhibiting a short-axis-oriented transition dipole moment.

1. Introduction

Spectroscopic properties of isolated molecules may be studied by a combination of supersonic jet expansion techniques and laser spectroscopy. Recently, the optical spectroscopy of substituted naphthalene molecules has received considerable attention due to an interesting variety of photophysical properties of these molecules. Several studies revealed a subtle dependence of the excited-state character, of the $S_1 - S_0$ transition dipole moment, of radiative lifetimes, and of vibrational state mixing in these aromatic molecules on the type of substitution, on the substitution site and on its conformation, as well as on the level of vibronic excitation employed.[1−12]

In the case of monosubstituted hydroxynaphthalenes (HN), a dramatic change in the acidity after $S_1 \leftarrow S_0$ excitation has promoted various laser spectroscopic studies. High-resolution experiments of 1-HN and 2-HN allowed for the correct assignment of the simultaneously present *cis* and *trans* isomers in a jet expansion, as well as the observation of the conformational dependence of the S_1-S_0 transition dipole moment orientation.[6] Dispersed fluorescence spectra of *trans*-1-HN also revealed the occurrence of extensive vibrational state mixing in the S_1 electronic state attributed to vibronically induced Duschinsky rotation.[10] Furthermore, incorporation of *trans*-1-HN into hydrogen-bonded cluster species with water and ammonia established the presence or absence of proton transfer as a function of cluster type and cluster size.[13,14]

The energy dependence of radiationless processes on the amount of vibrational excess energy in the S_1 electronic state was studied in the case of monosubstituted chloronaphthalenes (ClN), fluoronaphthalenes (FN), and methylnaphthalenes (MN).[4] While the 0^0 level nonradiative rates of these molecules vary strongly, the energy dependence of the nonradiative rates were found to be quite similar. In the case of 2-MN, vibrational mode mixing due to Duschinsky rotation in the S_1 electronic state was also observed at low excitation energy, comparable to the situation in *trans*-1-HN.[2,3]

We have recently begun a study of the photophysics and photochemistry of monosubstituted methoxynaphthalenes in order to investigate the role and importance of the methoxy group for their intramolecular energetics and dynamics.[15] The only methoxy substituted aromatic molecules studied spectroscopically in detail so far are methoxy substituted benzene (anisole)[16−19] and 4-methoxy-*trans*-stilbene.[20] In the case of anisole, the methoxy and methyl torsional frequencies were determined experimentally in the ground electronic state.[16,17] Extensive ab initio calculations of this molecule also revealed the planar geometry at the potential energy minimum in the ground electronic state, with a predicted barrier of $\approx$10 kJ/mol^{-1} to rotation of the methoxy group.[18,19] No experimental value for the methoxy torsion frequency was reported in the case of 4-methoxy-*trans*-stilbene, but the simultaneous presence of two ground state conformers in the molecular jet expansion was established by rotational coherence spectroscopy.[21]

In a previous publication[15] we presented first results concerning the identification of two isomeric ground state structures in the fluorescence excitation spectrum of jet-cooled 2-methoxynaphthalene (2MXN), tentatively assigned to the *cis* and *trans* configurations of the methoxy group relative to the long axis of the naphthalene subunit. Dispersed emission spectra of both vibronic origin bands were analyzed and compared with the corresponding spectrum of naphthalene. We also reported fluorescence lifetimes of various vibronic S_1 levels and first observations of vibrational quantum beats 978 cm^{-1} above the vibrationless S_1 level of *cis*-2MXN.[15]

In this paper we report a detailed analysis of single vibronic level fluorescence (SVLF) spectra following excitation of 25 levels in the vibronic $S_1 \leftarrow S_0$ spectrum of *cis*-2MXN. A fluorescence hole-burning technique was applied to establish excitation transitions due to the *cis* isomer. Assignments of ground state and excited state vibrational frequencies are given in comparison with results from ab initio calculations. The outcome of these ab initio frequency calculations and geometry

S1089-5639(98)00487-3 CCC: $15.00
Published on Web 05/28/1998

optimizations, which confirmed our previous assignments of the two isomers present, are also reported and discussed in detail.

2. Experimental Methods

Fluorescence excitation spectra of 2MXN (Fluka, >99%) were obtained using a mixture of 2MXN seeded in pure neon in a pulsed supersonic jet expansion with 1.5 bar stagnation pressure and 330 K nozzle temperature (0.35 mm nozzle orifice diameter). Excitation took place typically 20 mm downstream from the nozzle orifice by the output of a Nd:YAG pumped and frequency doubled pulsed dye laser (DCM in methanol). Total fluorescence was collected perpendicular to the nozzle/laser plane by a single quartz lens ($f = 150$ mm), focused onto a Hamamatsu R212 photomultiplier tube and recorded by a digital oscilloscope (Tektronix DSA-601).

Fluorescence hole-burning spectra were recorded with the same basic setup, additionally employing a second, separately pumped dye laser. In these experiments the high power output ($I \approx 400$ μJ) of the first dye laser (pump pulse) was scanned over the spectral region of interest. The low power output ($I \approx 40$ μJ) of the second, delayed dye laser (probe laser) was kept resonant with a fixed vibronic transition frequency of 2MXN. This probe laser pulse was delayed by 300 ns to the pump pulse using a DG-535 delay generator (Stanford Research Systems). The total fluorescence induced by the probe laser pulse was recorded as a function of the frequency of the scanning pump laser. Its intensity is directly proportional to the remaining population in the common ground state level after excitation by the pump pulse.[22]

Two experimental setups were employed to record dispersed fluorescence (DF) spectra. In both cases 2MXN was excited 10 mm downstream from the nozzle orifice ($X/D \approx 30$). Lower resolution spectra ($\Delta\bar{\nu} = 12$ cm^{-1}) of selected single vibronic levels (SVL) were obtained with a 1.0 m monochromator (SPEX 1704, holographic grating with 2400 lines/mm) and a Hamamatsu R-928 photomultiplier. Additionally, higher resolution spectra ($\Delta\bar{\nu} = 4-8$ cm^{-1}) of selected spectral regions of several SVL were recorded employing a 1.5 m monochromator (Sopra UHRS F1500, holographic grating with 1800 lines/mm) equipped with back-illuminated charge-coupled device (CCD) detector with 1752 by 532 pixels (Spectroscopy & Imaging GmbH, Erwitte, Germany). The CCD detector was cooled by liquid nitrogen down to 150 K, using a ST-130 controller unit (Princeton Instruments) connected to a personal computer. A typical spectrum was obtained after adding three separate 10 min exposures. Prior to addition, low-level background signals due to the presence of cosmic events were removed by a homemade computer program. Reported frequencies are accurate within ± 2 cm^{-1}.

3. Computational Methods

Full geometry optimizations and harmonic frequency calculations of *cis*-2MXN for the S_0 and S_1 electronic state were performed. Ground state calculations were done using the GAUSSIAN 92 package[23] on a RS/6000-320 workstation (64 MByte RAM), and excited state calculations were preformed on a RS/6000−540 machine (512 MByte RAM) using the GAUSSIAN 94 package.[23] The most stringent optimization criterion (OPT = VERYTIGHT) was used for the norm of the gradient in the case of the geometry optimizations. Convergence of the self-consistent field (SCF) was accomplished if the root mean square difference between the density matrix elements in successive cycles was less than 10^{-10} au (CONVER = 10). Additionally, no symmetry restrictions were applied. Our atom numbering scheme used for all geometry optimizations of *cis*-2MXN is illustrated in Figure 1a.

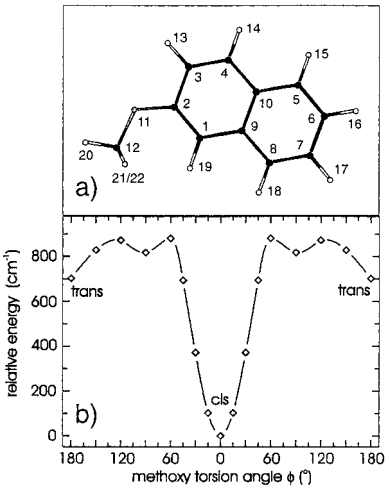

Figure 1. (a) Atom number scheme used in ab initio calculations of *cis*-2-methoxynaphthalene. See also Table 1 for the corresponding bond lengths and bond angles. (b) Plot of the relative total energy of 2MXN versus the dihedral angle ϕ ($C_1-C_2-O_{11}-C_{12}$) of the methoxy torsion as obtained by RHF/6-31G** single-point calculations (◇). The solid line is an interpolation curve calculated with a spline fit routine. See text for further details.

Electronic ground-state calculations were carried out at the restricted Hatree−Fock (RHF) level of theory using the 6-31G** basis set. A series of single-point ground state geometry optimizations was performed for different values of the dihedral angle ϕ ($C_1-C_2-O_{11}-C_{12}$) of the methoxy group relative to the naphthalene plane, in order to investigate the approximate potential energy surface along this internal coordinate. The single-excitation configuration interaction (CIS) method with the 6-31G** basis set was employed for the S_1 calculations. Direct SCF and direct CIS options were applied in these calculations. Although consideration of all singly excited configurations did not reproduce the correct excited state level order in CIS calculations of naphthalene[24−26] and β-methylstyrene,[27] the vibrational structure is determined mainly by the electronic distribution dominated by the singly excited configurations. Since our prime interest was in the vibrational level structure, we used the CIS method to provide estimates of vibrational S_1 frequencies of *cis*-2MXN.

4. Results of ab Initio Calculations

4.1. *cis*−*trans* Isomerization of 2MXN. As mentioned above, the first evidence of the presence of two conformational isomers in the jet-cooled fluorescence excitation and emission spectra of 2MXN was reported recently.[15] These conformers were tentatively assigned to the existence of *cis* and *trans* configurations of the methoxy group relative to the long axis of the naphthalene subunit. To investigate the simultaneous occurrence of different conformers in the electronic ground state of 2MXN, we performed partial geometry optimizations varying the methoxy dihedral angle ϕ ($C_1-C_2-O_{11}-C_{12}$) from 0° to 180° in 15° or 30° increments. Whereas the methoxy dihedral angle was kept fixed in these single-point calculations, all other internal coordinates were optimized at the RHF/6-31G** level of theory. The resulting one dimensional potential energy curve is given in Figure 1b. Although the continuous variation of an internal coordinate represents not necessarily a minimum energy path, all three local minima found with dihedral angles of ϕ = 0° (*cis* isomer), 90°, and 180° (*trans* isomer) located along this

torsional path were checked through harmonic frequency analyses to be real minima without any imaginary frequency mode.

The lowest potential energy point belongs to the *cis* isomeric configuration with a methoxy torsion angle $\phi = 0°$. This structure corresponds to the global potential energy minimum of the whole ground state potential energy surface (PES) of 2MXN, also obtained in a global geometry optimization without restriction of the methoxy dihedral angle (see section 4.2 below). As seen in Figure 1b the relative energy rises sharply between a methoxy torsional angle of $\phi = 0°$ and $\phi = \pm 50°$. On the other hand the potential energy of the *trans* configuration ($\phi = 180°$) is $\approx$700 cm^{-1} (8.4 kJ/mol) higher than the *cis* structure at this level of theory. As reported in ref 15, intensities of spectral features assigned to the *trans* isomer in the $S_1 \leftarrow S_0$ fluorescence excitation spectrum were considerably weaker than the corresponding vibronic transitions due to the *cis* isomer. Therefore, the substantial potential energy difference calculated for the two isomeric forms of 2MXN in the ground electronic state results in a considerably differing Boltzmann population factor in the supersonic jet expansion. This is most likely the reason for the large intensity difference observed.

The conformational preference of the *cis* configuration was also found in ^{1}H and ^{13}C nuclear magnetic resonance experiments of 2MXN in carbon tetrachloride solutions.[28] Proximate coupling between methyl and ring protons was used to determine the absolute conformation of the methoxy group. These results confirmed previous studies using carbon-13 chemical shift analysis, yielding an approximate population ratio of 19:1 between *cis* and *trans* isomer of 2MXN at 305 K. This indicates an enhanced stability of $\approx$ 4.8 kJ/mol of the *cis* configuration in the electronic ground state, which is in qualitative agreement with the results of our ab initio calculations.

Figure 1b also reveals a third local potential energy minimum along the methoxy torsional path in the ground electronic state. This third configuration with a methoxy torsion angle $\phi = 90°$, which was found to be a true minimum according to the harmonic frequency analysis, corresponds to a structural conformation with the methoxy group orthogonal to the aromatic ring system of the naphthalene subunit (i.e., an out-of-plane conformation). The well depth is very shallow, and the barrier to the *trans* configuration is almost negligible. The same sort of orthogonal local minimum structure was also reported in various ab initio calculations of methoxybenzene.[18,19] However Vincenz et al. [19] showed that this potential energy minimum of the orthogonal configuration of methoxybenzene disappeared after electron correlation effects were included through MP2/6-31G* calculations. We therefore expect that the same is true in the case of 2MXN. Further work is currently in progress to clarify this point.

4.2. Geometry Optimization of *cis*-2MXN in S_0 and S_1. Optimized internal coordinates of *cis*-2MXN, obtained by RHF/6-31G** calculations for the ground state S_0 and by CIS/6-31G** calculations for the first excited state S_1, are given in Table 1. Although no symmetry constraints were applied, deviations from planarity of the final geometries were negligible, yielding structures of overall C_s point group symmetry in both electronic states. Therefore, the methoxy group of the optimized structure lies in the plane of the naphthalene subunit in both electronic states, as shown in Figure 1a.

The calculated aromatic C−C bond lengths of *cis*-2MXN change only slightly under the influence of the methoxy substitution in the S_0 state, compared with calculated structural data obtained recently in the case of naphthalene.[26] None of the calculated C−C bond lengths in *cis*-2MXN differs by more than ±0.006 Å from its naphthalene counterpart. The optimized ground state value of the C_2-O_{11} bond length of *cis*-2MXN, which connects the methoxy group to the naphthalene subunit, is 1.347 Å. This value is noticeably shorter than a single C−O bond length in methyl ether, where a value of 1.43 Å is reported.[29] The shortening of the C_2-O_{11} bond length in *cis*-2MXN indicates a substantial double-bond character, induced by the connectivity to the aromatic subsystem. This shortening effect is less pronounced in the case of the second C−O bond in *cis*-2MXN, which involves the methyl group carbon atom. The calculated bond length of the $O_{11}-C_{12}$ bond is 1.399 Å, closer to the value of the C−O bond length in methyl ether, but still smaller. On the other hand, both optimized bond lengths for the two C−O bonds of *cis*-2MXN are very similar to results obtained for methoxybenzene using the RHF/6-31G* method. In this case, Vincenz et al.[19] reported a value of 1.350 Å for the $C_{Aromat}-O$ and 1.398 Å for the $O-CH_3$ bond length.

TABLE 1: Optimized Geometries of *cis*-2MXN in the Ground State S_0 and in the First Excited State S_1 Using the RHF/6-31G and CIS/6-31G** Method, Respectively**

bond	S_0 (Å)	S_1 (Å)	bond angle	S_0 (deg)	S_1 (deg)
$C_{10}-C_9$	1.407	1.453	$C_9-C_{10}-C_3$	118.3	118.5
$C_{10}-C_4$	1.424	1.405	$C_{10}-C_9-C_8$	118.6	119.1
C_9-C_8	1.419	1.407	$C_9-C_{10}-C_5$	119.4	117.8
$C_{10}-C_5$	1.417	1.399	$C_{10}-C_9-C_1$	118.3	118.3
C_9-C_1	1.425	1.396	$C_{10}-C_4-C_3$	121.2	122.3
C_4-C_3	1.352	1.402	$C_9-C_8-C_7$	120.8	121.6
C_8-C_7	1.360	1.408	$C_{10}-C_5-C_6$	120.8	121.5
C_5-C_6	1.360	1.414	$C_8-C_7-C_6$	120.5	119.1
C_7-C_6	1.413	1.377	$C_5-C_6-C_7$	119.9	120.9
C_1-C_2	1.360	1.425	$C_9-C_1-C_2$	120.1	121.3
C_3-C_2	1.423	1.380	$C_4-C_3-C_2$	120.3	119.1
C_2-O_{11}	1.347	1.338	$C_1-C_2-C_7$	120.3	120.4
$O_{11}-C_{12}$	1.399	1.403	$C_1-C_2-O_{11}$	125.5	122.7
C_4-H_{14}	1.076	1.076	$C_2-O_{11}-C_{12}$	119.5	121.2
C_8-H_{18}	1.076	1.076	$C_{10}-C_4-H_{14}$	118.9	118.7
C_5-H_{15}	1.076	1.076	$C_9-C_8-H_{18}$	119.0	118.8
C_1-H_{19}	1.073	1.073	$C_{10}-C_5-H_{15}$	118.9	119.3
C_3-H_{13}	1.074	1.073	$C_9-C_1-H_{19}$	118.3	118.7
C_7-H_{17}	1.076	1.074	$C_4-C_3-H_{13}$	121.8	121.5
C_6-H_{16}	1.076	1.076	$C_8-C_7-H_{17}$	120.0	120.0
$C_{12}-H_{20}$	1.086	1.085	$C_5-C_6-H_{16}$	120.4	118.8
$C_{12}-H_{21}$	1.086	1.085	$O_{11}-C_{12}-H_{20}$	111.4	111.5
$C_{12}-H_{22}$	1.080	1.080	$O_{11}-C_{12}-H_{21}$	111.4	111.5
			$O_{11}-C_{12}-H_{22}$	106.4	106.0

In the case of the first excited state S_1, our ab initio calculations of *cis*-2MXN showed a similar pattern of alternating aromatic C−C bond length increases and decreases, compared with their ground state values, as observed in the calculations of naphthalene[24,26] (see Table 1). For example, the C_9-C_{10} and C_3-C_4 bonds increased from 1.407 and 1.352 Å in S_0 to 1.453 and 1.402 Å in S_1, whereas the C_5-C_{10} and C_6-C_7 bonds decreased from 1.417 and 1.413 Å in S_0 state to 1.398 and 1.377 Å in S_1. As in naphthalene, these structural shifts are caused by bond order changes due to the $\pi-\pi^*$ excitation. The calculated bond lengths of the two C−O bonds of *cis*-2MXN were less affected by electronic excitation. Their predicted bond length changes are smaller than in the case of the aromatic carbon bonds. As seen from Table 1, a shortening of 0.009 Å was calculated for the C_2-O_{11} bond in S_1 compared with its S_0 value, whereas the calculated $O_{11}-C_{12}$ bond was slightly lengthened by 0.004 Å after excitation.

Calculated bond angles of *cis*-2MXN are also given in Table 1 for the S_0 and S_1 electronic states. As observed in the case of methoxybenzene,[18,19] there is substantial steric hindrance in the S_0 state between methyl group hydrogen atoms and the close

lying hydrogen atom H_{19}, which is connected to the aromatic subsystem (see Figure 1a). Firstly, instead of an unperturbed $C_1-C_2-O_{11}$ angle of 120°, this angle increases to 125.5° in the optimized ground state geometry. It decreases slightly to 122.7° in the optimized excited state geometry. Secondly, the preferred orientation of the methyl group also provides evidence for significant steric interactions. The calculated orientation is different for that expected on the basis of electronic considerations alone, whereby the eclipsing $C_{12}-H_{20}$ bond should point *toward* the ring. Thirdly, the angle $C_2-O_{11}-C_{12}$ is strongly perturbed. In the case of an idealized sp^3 hybridized oxygen atom, a value of 109.7° is expected. The calculated values are 119.5° in S_0 and 121.2° in S_1, indicating that the oxygen atom exhibits considerable sp^2 character in both electronic states. This sp^2 hybridization is additionally favored by the planar structure of *cis*-2MXN.

In summary, our calculations predict that the equilibrium structure of *cis*-2MXN does not change significantly after S_0-S_1 electronic excitation, maintaining a planar C_s symmetry. The rotational constants remain comparable in both electronic states. Their calculated values are $A'' = 2.3822$, $B'' = 0.6246$, and $C'' = 0.4964$ GHz for the ground electronic state and $A' = 2.3350$, $B' = 0.6216$, and $C' = 0.4924$ GHz for the first excited state.

4.3. S_1-S_0 Transition Dipole Moment Orientation. Using the CIS procedure in the excited state calculations, dominant contributions of the S_1 state wavefunction of *cis*-2MXN are due to two electronic configurations, both involving $\pi-\pi^*$ single electron excitations. The leading configuration arises from a single electron excitation out of the highest occupied molecular orbital (HOMO) to the lowest unoccupied molecular orbital (LUMO). The second, smaller term originates from a single electron excitation out of the HOMO-1 orbital to the LUMO+1 orbital (i.e., a $(HOMO-1)^1$ $(LUMO+1)^1$ configuration). Furthermore, the calculated S_2 state wave function consists of the two main single excitation configurations $(HOMO-1)^1$ $(LUMO)^1$ and $(HOMO)^1$ $(LUMO+1)^1$. The calculated energy difference between S_1 and S_2 is approximately 2900 cm^{-1}.

On the other hand, the S_1 state of naphthalene is known to consist of a linear combination of the $(HOMO-1)^1$ $(LUMO)^1$ and $(HOMO)^1$ $(LUMO+1)^1$ configurations, whereas the S_2 state consists of the $(HOMO)^1$ $(LUMO)^1$ configuration.[6] Since the $(HOMO)^1$ $(LUMO)^1$ configuration is the leading term in the S_1 state of *cis*-2MXN, this electronic state correlates with the S_2 state of parent naphthalene, and the S_2 state of *cis*-2MXN can be correlated to the S_1 state of naphthalene. Clearly, our CIS calculations predict a state inversion between S_1 and S_2 state in *cis*-2MXN in comparison with naphthalene.

The calculated energy difference between the S_0 and S_1 electronic states of *cis*-2MXN in their optimized geometries is 5.101 eV. The energy of the 0−0 transition is found by correcting the energy difference between the two electronic states for changes in the zero-point energy (ZPE). Using the calculated frequencies (see below), a theoretical value of 40060 cm^{-1} is obtained. This is considerably larger than the experimentally determined value of 31028 cm^{-1}.[15] The predicted oscillator strength of the $S_1 \leftarrow S_0$ excitation is $f = 0.1334$, indicating a relatively strong transition in agreement with experiment. This oscillator strength is of the same order of magnitude as the oscillator strength of the $S_2 \leftarrow S_0$ excitation in naphthalene. Furthermore, the $S_2 \leftarrow S_0$ transition in naphthalene is short-axis (b-type) polarized, whereas its $S_1 \leftarrow S_0$ transition is long-axis (a-type) polarized. Projecting the calculated transition dipole moment of the $S_1 \leftarrow S_0$ excitation of *cis*-2MXN onto a naphthalene fixed axis system yields an almost completely short-axis-polarized transition moment, with an angle of only 16° between the $S_1 \leftarrow S_0$ transition dipole moment and the short axis of the naphthalene subunit. Therefore, a hybrid band type of approximately 90% b-type character and 10% a-type character is predicted from our CIS calculations in the case of origin excited *cis*-2MXN. This situation in *cis*-2MXN is similar to results obtained for *cis*-2HN, where Johnson et al. found a predominantly b-type-polarized $S_1 \leftarrow S_0$ transition dipole moment.[6] These authors clearly showed that the σ/π mixing between the oxygen lone pair and the naphthalene orbitals is responsible for this observed rotation of the transition dipole moment compared to parental naphthalene.

4.4. Harmonic Frequencies of *cis*-2MXN in S_0 and S_1. Beside optimized minimum energy structures, harmonic frequencies were also calculated for both electronic states of *cis*-2MXN. Analytical second derivatives were used in both cases. *cis*-2MXN has 60 normal modes. Using C_s symmetry the 41 in-plane modes are totally symmetric (a′ modes) and the 19 out-of-plane modes are nontotally symmetric (a″ modes).

The results of the harmonic frequency analyses are given in Table 2. All modes are ordered after their symmetry and with decreasing frequency in the S_0 state. Note that we calculated the Duschinsky matrix from the given normal mode vectors in both electronic states in order to assign the excited state vibrations to the correct ground state vibrations, which is the reason that the excited state frequencies in Table 2 are not ordered after their frequencies. Also given are the calculated harmonic displacement vectors ΔQ for all in-plane modes. Calculating relative frequency changes between the two electronic states showed that out-of-plane frequencies are predicted to change on the order of 5−10%, whereas in-plane modes only change on the order of 2−5% after excitation. Therefore, overtone transitions of out-of-plane vibrations are expected to show up in the vibronic $S_1 \leftarrow S_0$ spectrum of *cis*-2MXN. Detailed assignments of the experimental frequencies to the calculated ones will be discussed below.

The scaled frequencies of the methoxy torsion (ν_{60}), the methyl torsion (ν_{57}), and the methoxy in-plane bending vibration (ν_{41}) are calculated to 72, 237, and 189 cm^{-1} in S_0. Their ground state atomic vector displacements are reproduced in Figure 2. Thereby, the methoxy torsion is the lowest energetic out-of-plane mode, and the methoxy in-plane bending mode the lowest energetic in-plane mode of *cis*-2MXN. The frequencies of the methoxy and methyl torsion of *cis*-2MXN are very similar to results obtained in ab initio calculations of methoxybenzene, where scaled frequencies of 75 cm^{-1} for the methoxy and 200 cm^{-1} for the methyl torsion were found.[19] This indicates that both potential energy hypersurfaces have similar curvatures along these two coordinates, at least close to the potential energy minimum. Furthermore, the relatively high frequency of the methyl torsional mode ν_{57} also shows that the steric hindrance between the neighboring hydrogen atoms H_{19} and H_{21}/H_{22} (see Figure 1a) is considerably large, leading to a hindered methyl rotor motion.

5. Experimental Results

5.1. Excitation Spectroscopy. *5.1.1. Unsaturated Fluorescence Excitation.* In ref 15 we presented a fluorescence excitation (FEX) spectrum of *cis*-2MXN which was partially saturated in a few major transitions in order to show weaker vibronic bands, as well as to reveal the very weak features caused by the presence of the *trans*-2MXN isomer. Therefore, we reproduce in Figure 3 a fluorescence excitation spectrum recorded under very low laser power conditions to avoid any

TABLE 2: Theoretical In-plane (a′) and Out-Of-Plane (a″) Vibrational Frequencies of *cis*-2MXN in the Electronic Ground State S_0 and in the First Excited State S_1 Using the RHF/6-31G and CIS/6-31G** Methods[a]**

	mode	S_0 frequency (cm^{-1})	S_1 frequency (cm^{-1})	displacement ΔQ
a′	1	3043	3050	−0.015
	2	3042	3054	0.025
	3	3032	3042	0.031
	4	3019	3025	0.000
	5	3012	3016	0.019
	6	3005	3011	−0.013
	7	3000	3008	0.004
	8	2972	2978	0.002
	9	2922	2930	0.000
	10	2863	2868	−0.005
	11	1659	1419	0.154
	12	1630	1470	0.025
	13	1606	1435	−0.109
	14	1511	1528	−0.084
	15	1483	1500	−0.022
	16	1479	1477	0.025
	17	1450	1452	0.039
	18	1441	1396	0.066
	19	1376	1366	−0.440
	20	1351	1326	0.430
	21	1324	1308	−1.346
	22	1261	1276	−0.700
	23	1246	1255	−0.041
	24	1215	1199	−0.189
	25	1191	1166	−0.273
	26	1163	1116	−0.423
	27	1140	1037	0.249
	28	1115	1063	0.139
	29	1077	1177	−0.103
	30	1049	1053	0.084
	31	992	993	−0.302
	32	937	908	0.164
	33	884	865	0.101
	34	756	718	−0.238
	35	683	665	−0.080
	36	611	582	0.089
	37	509	500	0.508
	38	495	472	−0.831
	39	421	397	−0.396
	40	333	329	−0.149
	41	189	190	0.461
a″	42	1468	1470	
	43	1159	1153	
	44	1005	932	
	45	991	875	
	46	975	864	
	47	885	816	
	48	859	797	
	49	827	736	
	50	760	672	
	51	756	700	
	52	647	584	
	53	535	481	
	54	478	390	
	55	401	335	
	56	313	266	
	57	237	214	
	58	183	151	
	59	129	115	
	60	72	55	

[a] All frequencies are scaled by a common scaling factor of 0.9. We also give the predicted normal coordinate displacements ΔQ of all in-plane modes in the case of a S_1-S_0 vibronic excitation, which were calculated from the Cartesian normal coordinate vector components of both electronic states.

saturation effects. Figure 3 shows that the origin transition of *cis*-2MXN at 31028 cm^{-1} is the strongest band in the whole vibronic system, indicating the allowed character of this $\pi-\pi^*$ excitation. Beside the origin band, about a dozen more transitions are clearly visible to the higher energy side of the spectrum. Most of these bands could be correlated to naphthalene like totally symmetric modes as given in Table 1 of ref 15.

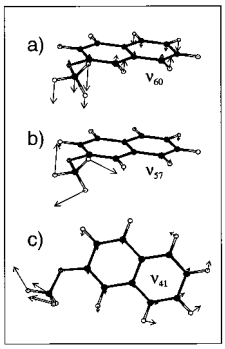

Figure 2. The atomic vector displacements of three low frequency skeletal vibrations of *cis*-2MXN. ν_{60} in (a) corresponds to the methoxy torsion, ν_{57} in (b) to the methyl torsion, and ν_{41} in (c) to the methoxy in-plane bending mode.

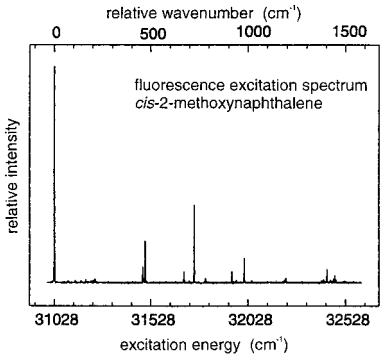

Figure 3. Unsaturated fluorescence excitation spectrum of jet-cooled *cis*-2MXN. Transitions are also measured relative to the origin band at 31028 cm^{-1}.

5.1.2. Hole-burning Spectrum. To confirm that all features appearing in Figure 3 and in Figure 1 of ref 15 belong to the *cis* isomer of 2MXN, we also recorded a fluorescence hole-burning (HB) spectrum using two independently pumped dye lasers. A first pump laser pulse depleted the vibrationless ground state. A second laser pulse at fixed frequency subsequently probed the remaining population in the common ground state level. The frequency of this probe laser was set to the origin transition at 31028 cm^{-1}. Figure 4 shows the resulting HB spectrum (upper trace) of *cis*-2MXN, together with a simultaneously recorded (saturated) fluorescence excitation spectrum (lower trace). As seen in Figure 4, all stronger features apparent in the fluorescence excitation spectrum are also present in the HB spectrum. This proves that all vibronic transitions shown in the excitation spectra of Figure 3 and Figure 4 (lower trace) belong to the same molecular species and originate from the same ground state level. Therefore, all of these bands were assigned to belong to the *cis*-2MXN isomer.

Figure 5 shows a second HB spectrum, obtained by scanning the red-shifted frequency region of the *trans*-2MXN isomer with the strong pump laser while fixing the probe laser at 30368 cm^{-1}. This transition was previously assigned to the origin band of the $S_1 \leftarrow S_0$ transition of *trans*-2MXN (see Figure 1 in ref 15). The upper trace in Figure 5 shows again the HB spectrum, and the lower trace the simultaneously recorded FEX spectrum. The observed coincidence of dip features in the HB spectrum with transitions present in the FEX spectrum indicates their

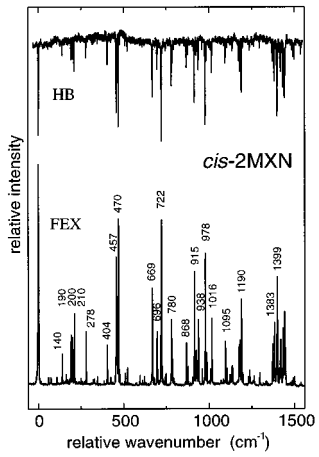

Figure 4. Fluorescence hole-burning spectrum (upper trace) and saturated fluorescence excitation spectrum (lower trace) of *cis*-2MXN. Transitions are measured relative to the origin band at 31028 cm^{-1}.

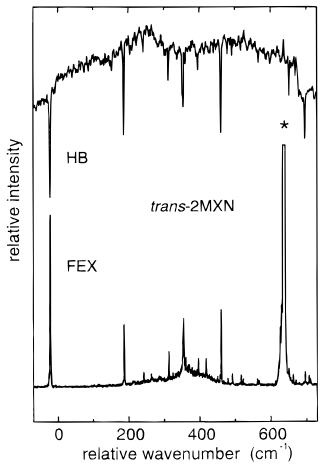

Figure 5. Fluorescence hole-burning spectrum (upper trace) and saturated fluorescence excitation spectrum (lower trace) of *trans*-2MXN. Transitions are measured relative to the origin band at 30368 cm^{-1}. Note that the strong origin transition of *cis*-2MXN in the excitation spectrum at 660 cm^{-1} (*) is missing in the hole-burning spectrum.

connectivity through their common ground-state level. On the other hand, note that the strong excitation band 660 cm^{-1} to the blue of the origin transition of *trans*-2MXN, which corresponds to the origin band of the *cis* isomer, is completely absent in the HB spectrum of the *trans* isomer. This demonstrates that the two vibronic systems are independent of each other (i.e., they originate from two distinct isomers of 2MXN). In the following we will concentrate on the *cis* isomer, because the very weak excitation features of the *trans* isomer did not allow for a more detailed analysis of their dispersed fluorescence spectra further than already reported in ref 15.

5.2. Single Vibronic Level Fluorescence (SVLF) Spectra. To obtain ground-state vibrational frequencies of *cis*-2MXN, an extensive set of SVLF spectra was recorded, following excitation of 25 vibronic bands in its FEX spectrum. In the following, we report in detail our experimental results for the different SVLF spectra recorded up to approximately 1700 cm^{-1} of vibrational energy in S_1. The obtained set of experimental frequencies will be compared in section 6 with theoretical results from our ab initio study.

5.2.1. Origin Dispersed Fluorescence. The SVLF spectrum following excitation of the 0_0^0 level of *cis*-2MXN is reproduced in Figure 6. The spectral resolution is 6 cm^{-1}, and the spectrum was obtained using the liquid nitrogen cooled CCD camera setup as described in section 2. Table 3 lists most of the observed transitions up to 1800 cm^{-1} of vibrational energy in the ground electronic state. The labels used refer to the fundamental modes as obtained from our ab initio calculations, whereby ν_1 to ν_{41}

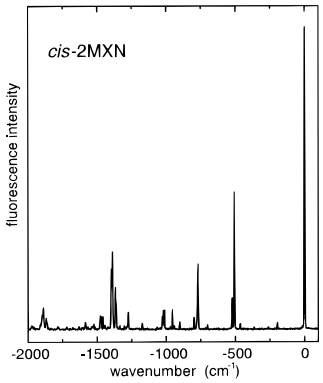

Figure 6. Dispersed SVLF spectrum following origin excitation of *cis*-2MXN. Transitions are measured relative to the excitation position at 31028 cm^{-1}. Assignments are given in Table 3.

TABLE 3: Frequencies, Intensities and Proposed Assignments of Transitions in the SVLF Spectrum Following $S_1 \leftarrow S_0$ Origin Excitation of *cis*-2MXN[a]

frequency (cm^{-1})	intensity	assignment	frequency (cm^{-1})	intensity	assignment
0	100	origin	1279	5	$38_1^0\,34_1^0$
160	<1	60_2^0	1288	<1	?
196	2	41_1^0	1294	<1	$37_1^0\,34_1^0$
211	<1	59_2^0	1307	1	?
262	1	$60_1^0\,58_1^0$	1322	<1	?
364	1	58_2^0	1335	<1	?
420	<1	$60_3^0\,58_1^0$	1341	1	?
432	<1	39_1^0	1357	1	?
464	2	57_2^0	1367	8	(20_1^0)
508	43	38_1^0	1373	14	?
523	10	37_1^0	1394	23	(19_1^0)
623	<1	36_1^0	1398	13	?
703	1	35_1^0, $41_1^0\,38_1^0$	1403	20	(18_1^0)
718	<1	$59_2^0\,38_1^0$	1426	1	?
772	16	34_1^0	1448	2	?
777	6	$(58_3^0\,57_1^0)$	1464	4	$38_1^0\,32_1^0$
783	2	$60_1^0\,58_1^0\,37_1^0$	1476	4	$35_1^0\,34_1^0$
800	3	$(59_1^0\,57_1^0\,38_1^0)$	1483	4	?
871	<1	$58_2^0\,38_1^0$	1521	1	38_3^0
884	<1	$58_1^0\,37_1^0$	1530	2	$38_1^0\,31_1^0$
904	2	33_1^0	1537	1	?
943	1	54_2^0	1541	1	?
955	6	32_1^0	1545	1	34_2^0
972	1	$41_1^0\,34_1^0$	1568	<1	37_3^0
1015	6	38_2^0	1578	1	?
1023	6	31_1^0	1592	3	?
1030	4	$38_1^0\,37_1^0$	1608	<1	?
1045	<1	37_2^0	1612	<1	?
1068	1	53_2^0	1617	1	?
1124	<1	(28_1^0)	1638	1	?
1177	2	(26_1^0)	1674	<1	$34_1^0\,33_1^0$
1202	<1	$39_1^0\,34_1^0$	1683	1	$38_1^0\,26_1^0$
1210	<1	$38_1^0\,35_1^0$	1727	1	$34_1^0\,32_1^0$
1216	<1	(29_1^0)	1785	<1	?
1224	<1	$37_1^0\,35_1^0$	1793	1	$34_1^0\,31_1^0$

[a] Frequencies are accurate to within ±2 cm^{-1}. Parenthesis indicate more tentative assignments.

correspond to in-plane (a′) vibrations, and ν_{42} to ν_{60} to out-of-plane (a″) vibrations. Table 3 indicates that most features having an intensity greater than 1% of the 0_0^0 transition could be assigned, as well as a significant number of weaker bands. Compared with Table 3 of ref 15 we were able to distinguish considerably more transitions in this work due to an increased resolution and a higher sensitivity of the experimental setup. This led to the appearance of several close lying multiplets of various bands which were not resolved in our previous study, especially in the region above 1000 cm^{-1} of vibrational energy in S_0.

Beside the 0_0^0 band, which is the strongest band in this spectrum, three transition frequencies dominate the SVLF spectrum following origin excitation. Their frequencies are 508, 772, and 1394 cm^{-1} below the excitation wavelength. All three bands form small progressions (seen up the $n \leq 3$), and they are dominantly present in combination bands with other optically active modes. The two modes with fundamental frequencies of 772 (ν_{34}) and 1394 cm^{-1} (ν_{19}) correlate most likely to the totally symmetric naphthalene modes ν_8 (a_g, 761 cm^{-1}) and ν_5 (a_g, 1380 cm^{-1}).[24] Each of these two vibrations are also strongly Franck−Condon (FC) active in the SVLF spectrum of origin excited naphthalene.[30,31] In the case of *cis*-2MXN, the band at 1394 cm^{-1} seems to be a member of a complicated multiplet structure of at least five levels, having frequencies of 1367, 1374, 1394, 1398, and 1403 cm^{-1}. It is highly unlikely that all five transitions represent nearly degenerate $\Delta v = 1$ transitions of in-plane fundamental modes. Some of them may belong to combination bands which gain their intensity through a multi-level Fermi resonance with the 1394 cm^{-1} band.

The assignment of the third strong feature in the origin excited SVLF spectrum of *cis*-2MXN at 508 cm^{-1} is not completely resolved. It could correlate either to the parental naphthalene mode $\nu_{\bar{8}}$ (b_{3g}, 508 cm^{-1}), or to the nearby, totally symmetric mode ν_9 (a_g, 514 cm^{-1}). In the case of naphthalene, mode $\nu_{\bar{8}}$ can only gain intensity through Herzberg−Teller (HT) coupling. This is no longer true for the reduced symmetry of *cis*-2MXN, because b_{3g} modes in D_{2h} correlate to a′ modes in C_s. As seen in Figure 6, the transition at 508 cm^{-1} is actually accompanied by a weaker band at 523 cm^{-1}. Therefore it seems that both naphthalene like modes appear in the SVLF spectrum of *cis*-2MXN following origin excitation. Compared with our ab initio calculations, and due to further reasons given below, we assign the 508 cm^{-1} band to mode ν_{38} of *cis*-2MXN, correlating most likely with the naphthalene mode $\nu_{\bar{8}}$ (b_{3g}), and the 523 cm^{-1} band to mode ν_{37}, which may correspond to mode ν_9 (a_g) of naphthalene.

Beside these three strongly FC active modes, we could assign several more bands to originate from fundamental ($\Delta v = 1$) or overtone ($\Delta v = 2$) transitions, revealing ground state frequencies of the corresponding vibrations involved. Transitions with the most firmly established assignments consist of ground-state modes with frequencies of 80, 106, 182, 196, 232, and 703 cm^{-1}. All of them also appear as members of various combination bands with totally symmetric modes (see Table 3). Furthermore, transitions at 904, 955, 1023, 1177, 1364, and 1403 cm^{-1} are tentatively assigned to fundamental $\Delta v = 1$ transitions of totally symmetric modes. These assignments are less firmly established from the origin excited SVLF spectrum due to the increasing density and congestion of observed features.

5.2.2. Low-Energy Modes with E_{vib} (S_1) ≤ 404 cm^{-1}. Figure 7 shows the SVLF spectra following excitation of the six vibronic bands 140, 190, 200, 210, 278, and 404 cm^{-1} above the $S_1 \leftarrow S_0$ origin transition of *cis*-2MXN (see also Figure 4).

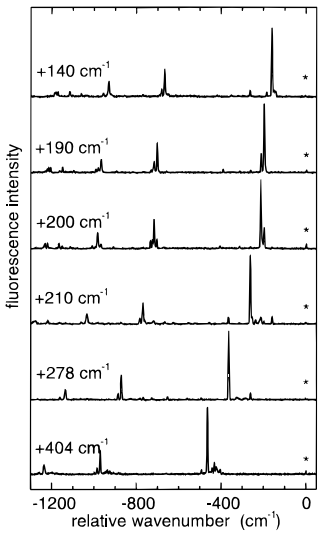

Figure 7. Dispersed SVLF spectra obtained following excitation of bands 140−404 cm^{-1} vibrational energy in S_1 of *cis*-2MXN. Transitions are measured relative to the excitation position which is indicated by an asterisk in each case.

The major progression seen in each of these SVLF spectra are 160, 196, 211, 262, 364, and 464 cm^{-1}. All these frequencies also appear as fundamental or overtone transitions in the SVLF spectrum following origin excitation. Furthermore, all SVLF spectra shown in Figure 7 look very similar to the corresponding spectrum of the origin band (compare with Figure 6). Built onto a dominant $\Delta v = 0$ transition, which serves as a false origin band, other totally symmetric progressions and combination bands appear, as observed in the SVLF spectrum of the origin transition.

The excitation 190 cm^{-1} above the S_1 origin transition is assigned to the in-plane bending mode of the methoxy group, ν_{41}. This is the lowest in-plane mode of 2MXN. Its ground state frequency is 196 cm^{-1} as obtained from its SVLF spectrum. The four excitations at 140, 200, 278, and 404 cm^{-1} above the $S_1 \leftarrow S_0$ origin transition are assigned to overtone bands $\Delta v = 2$. Their corresponding ground state mode frequencies are 80 (ν_{60}), 106 (ν_{59}), 182 (ν_{58}), and 232 cm^{-1} (ν_{57}). The excitation at 210 cm^{-1} in S_1 is assigned to a combination band of ν_{60} and ν_{58}. This is consistent with the measured frequency of 262 cm^{-1} below the excitation energy of the $\Delta v = 0$ ($60_1^1 58_1^1$) false origin transition in its SVLF spectrum.

A closer look at individual SVLF spectra in Figure 7 indicates that all six traces show the clear signatures of vibrational mode mixing despite the low energy of the vibrational modes involved. First, the false origin transitions of modes ν_{41} and ν_{59} appear as doublets of interchangeable frequencies, indicating that the excited single vibronic levels 41^1 and 59^2 are mixtures of each other, coupled by a Fermi resonance in the excited state. Second, the SVLF spectra of the levels 60^2 and 58^2 contain additional weak features in the vicinity of their $\Delta v = 0$ bands, which can be assigned to $60_0^2 58_2^0$ and $58_0^2 60_2^0$ transitions. These features are typical crossed sequence transitions of the form $A_0^n B_n^0$ due to Duschinsky rotation. Thirdly, the SVLF spectrum of the 404 cm^{-1} band (57_0^2) shows the appearance of a low intensity "bump" to the blue side of its false origin transition, also indicating the presence of vibrational mixing. Using an experimental setup with approximately 6 cm^{-1} resolution, individual features at 391, 404, 424, 432, and 442 cm^{-1} below the excitation energy could be resolved. The first three bands are assignable as $57_0^2 41_2^0$, $57_0^2 41_1^0 59_2^0$, and 57_0^2

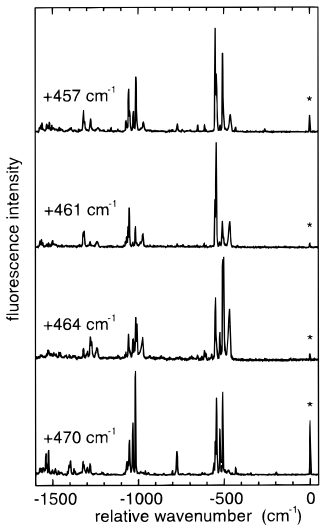

Figure 8. Dispersed SVLF spectra obtained following excitation of bands 457−470 cm^{-1} vibrational energy in S_1 of *cis*-2MXN. Transitions are measured relative to the excitation position which is indicated by an asterisk in each case.

59_4^0 transitions, revealing some weak state mixing involving mode ν_{57} and mode ν_{59}. The assignments of the other two bands at 432 and 442 cm^{-1} are yet unknown, although the band at 432 cm^{-1} belongs most likely to a fundamental $\Delta\nu = 1$ transition of mode ν_{39}, also seen in other SVLF spectra (see below).

5.2.3. Modes with Energy $E_{vib}(S_1) \approx 460 \pm 10$ cm^{-1}. At least six close lying bands are visible within 20 cm^{-1} in the FEX and HB spectra reproduced in Figure 4 in the spectral region approximately 460 cm^{-1} above the $S_1 \leftarrow S_0$ origin transition of *cis*-2MXN. Figure 8 shows the SVLF spectra of the four strongest excitation bands in this spectral region, with 457, 461, 464, and 470 cm^{-1} vibrational energy in S_1. These spectra reveal a case of extensive vibrational state mixing in the low energy region of the first excited state of *cis*-2MXN. Similar examples of considerable vibrational state mixing in substituted naphthalenes were also observed recently at low vibrational energy in S_1 in the case of 2-methylnaphthalene[2,3] and 1-hydroxynaphthalene.[10]

Each emission spectrum reproduced in Figure 8 shows a multiplet of up to 10 individual transitions in its false origin region. Built on these multiple false origin features are combination bands with totally symmetric modes as known from the origin excited SVLF spectrum. At the false origin position five common, strong and sharp features appear at 502, 508, 523, 543, and 551 cm^{-1} in all four spectra, as well as a broad feature centered at 467 cm^{-1}, clearly seen in three of the four spectra shown. Weaker common features appear at 422, 432, 454, 464, 476, and 559 cm^{-1} below the excitation energy.

Two of the stronger emission bands, at 508 and 523 cm^{-1}, respectively, were already apparent in the SVLF spectrum after origin excitation as mentioned above. The 508 cm^{-1} feature is the most FC active vibration in this energy region. Its S_1 frequency is 470 cm^{-1}, as seen from the lowest trace of Figure 8. We assigned this vibration to the in-plane mode ν_{38} of *cis*-2MXN. Beside the acceptable agreement between the experimental and calculated frequency, the ab initio calculations also predicted a large displacement between the ground and excited electronic state in this normal coordinate (see Table 2), which is observed experimentally. Furthermore, all four SVLF spectra reproduced in Figure 8 show strong transitions terminating in the S_0 levels 38_1 and 38_2. This reveals that these bands gain their intensity in S_1 through a coupling with mode ν_{38}.

The excited state frequency of the second vibration already appearing in the origin excited SVLF spectrum, with a S_0 frequency of 523 cm^{-1}, was found in a relatively weak band 476 cm^{-1} above the S_1 origin. We assigned this vibration to the in-plane mode ν_{37}. Again, the calculated frequency in S_0 and S_1 are in good agreement with experiment.

The SVLF spectra of the strong excitation bands at 457, 461, and 464 cm^{-1} could not be assigned to originate from other in-plane modes. No corresponding $\Delta\nu = 1$ transition was observed in the origin excited SVLF spectrum, and our ab initio calculations also did not predict additional in-plane modes in this spectral region. Therefore, we tentatively assign these three excitation bands to originate from out-of-plane combination bands. These assignments are supported by the SVLF spectra shown in Figure 8 through the observation of various out-of-plane combination bands. For example, transitions terminating in the ground-state overtone levels 59_2, 58_2, and 57_2 at 211, 363, and 464 cm^{-1} are seen. Further peaks indicating the involvement of out-of-plane modes are bands at 260, 312, 611, and 651 cm^{-1}, which could be assigned to the terminating S_0 levels 60_159_1, 60_157_1, $60_157_141_1$, and $60_158_141_1$, respectively. The two strong emission features seen in all four SVLF spectra with frequencies of 501 and 550 cm^{-1} below excitation wavelength could also tentatively be assigned to transitions terminating in the ground state levels 59_358_1 and $60_159_141_1$, respectively. Using this information together with the low energetic frequencies established for ν_{60} to ν_{57}, three out-of-plane combination levels were found with frequencies of 460−470 cm^{-1} in S_1, which may be responsible for the observed congestion in this spectral region. These are the combination levels $60^157^141^1$ at 464 cm^{-1}, 58^241^1 at 470 cm^{-1}, and 60^159^2-57^1 at 472 cm^{-1} in S_1. The presence of modes ν_{60} and ν_{58} in most of these transitions may indicate the active role of both vibrations in the coupling of the various levels at this internal energy in S_1 of *cis*-2MXN. As mentioned above, ν_{60} corresponds to the methoxy torsion mode (see Figure 2a), and mode ν_{58} is the lowest energetic out-of-plane mode which correlates to a parental naphthlene mode. This mode can be assigned to a C−H wagging vibration of a_u symmetry in naphthalene.

The assignment of the broad emission feature centered at 467 cm^{-1} below the excitation wavelength (see Figure 8) could not be resolved completely. Allowed transitions in this spectral region, and therefore possible assignments, are bands with terminating levels 57_2 (464 cm^{-1}) and 60_357_1 (471 cm^{-1}) in S_0. Although taking spectra with a resolution up to $\Delta\bar{\nu} = 5$ cm^{-1}, we could not yet resolve this emission band into individual components. It remains unclear if there is a dynamical process involved in the apparent broadening of this transition. Also not resolved is the question of the involvement of mode ν_{56} in several emission features. Using the calculated frequency of 313 cm^{-1}, bands at 417 (weak), 543 (strong), and 623 cm^{-1} (medium) could be explained as out-of-plane combination transitions terminating in the S_0 levels 59_356_1, 57_356_1, and 56_2, respectively. This reveals an experimental frequency $\nu_{56}(S_0)$ of 311 cm^{-1}, in good agreement with the calculated value of 313 cm^{-1}. Nevertheless, because no other transitions were observed involving mode ν_{56}, its assignment remains inconclusive.

5.2.4. Modes with Energy $E_{vib}(S_1) = 669-978$ cm^{-1}. In Figures 9 and 10, the SVLF spectra following excitation of bands with 669 to 978 cm^{-1} vibrational energy in S_1 are shown. Several features are evident from these spectra. First, all spectra

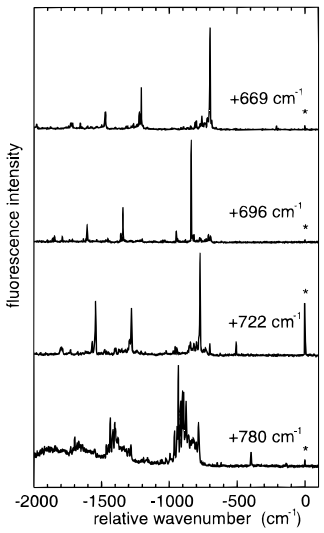

Figure 9. Dispersed SVLF spectra obtained following excitation of bands 669 to 780 cm^{-1} vibrational energy in S_1 of *cis*-2MXN. Transitions are measured relative to the excitation position which is indicated by an asterisk in each case.

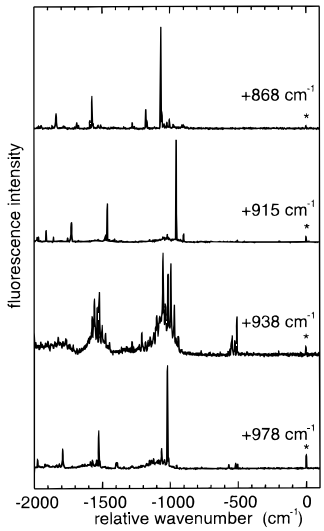

Figure 10. Dispersed SVLF spectra obtained following excitation of bands 868−978 cm^{-1} vibrational energy in S_1 of *cis*-2MXN. Transitions are measured relative to the excitation position which is indicated by an asterisk in each case.

beside the two traces with 780 and 938 cm^{-1} internal energy above S_1 show well resolved, sharp emission features, mostly out of a single vibronic level. Second, these spectra reveal either a small amount of unresolved, relaxed emission features in the vicinity of the main false origin transition (see for example the traces from levels 669 and 722 cm^{-1} in Figure 9, and 978 cm^{-1} in Figure 10), or a few sharp, crossed sequence transitions in the same spectral region. Two crossed sequence transitions are especially evident in the SVLF spectrum of the 722 cm^{-1} level, 508 and 701 cm^{-1} below the excitation frequency. Duschinsky rotation seems to couple mode ν_{38} (508 cm^{-1}) and ν_{35} (701 cm^{-1}) to mode ν_{34}, which has a S_0 frequency of 772 cm^{-1}. The corresponding transition $38_0^1\,34_1^0$ is also visible in the SVLF spectrum of mode ν_{38} (470 cm^{-1} in S_1) at 772 cm^{-1}, as seen in Figure 8. In the case of SVLF spectrum excited at 868 cm^{-1}, prominent crossed sequence transitions show up at 1004, 1021, 1177, and 1276 cm^{-1}, but none of these frequencies are observed in other SVLF spectra up to this vibrational energy in S_1.

Strong features in the false origin regions of the various spectra shown in Figures 9 and 10, which also appear as possible $\Delta v = 1$ transitions in the origin excited SVLF spectrum, are assigned to in-plane modes of *cis*-2MXN. This is the case for the frequencies at 701, 772, 904, 954, and 1177 cm^{-1}. They were assigned to the ground state modes ν_{35}, ν_{34}, ν_{33}, ν_{32}, and ν_{26}, respectively, also by comparison with the ab initio results. Thereby, ν_{34} with a ground state frequency of 772 cm^{-1} is one of three strongest FC active modes in *cis*-2MXN. Aside from showing a long progression in its SVLF spectrum, it also appears dominantly in the origin excited SVLF spectrum and in various combination bands. Its large FC factor is in qualitative agreement with the calculated value for the displacement of the potential energy surfaces along this normal coordinate (see Table 2).

The emission spectra taken from excitations 696 and 868 cm^{-1} above the S_1 origin level reveal large, relative frequency changes between the ground and first excited electronic state of approximately 18% (see Figure 10). This is much larger than calculated for any in-plane vibration. If both these two frequencies would belong to in-plane modes, prominent progressions with these frequencies would appear in the origin excited SVLF spectrum as well as in the FEX spectrum, which is not the case. On the other hand, several out-of-plane modes are calculated to show large frequency changes going from S_0 to S_1, and therefore we assign the excitation frequencies at 696 and 868 cm^{-1} to originate from out-of-plane overtone excitations. More specifically, the bands at 696 and 868 cm^{-1} in the FEX spectrum are assigned to the transitions 55_0^2 and 53_0^2 in comparison with their calculated S_1 frequencies (see Table 2). From the corresponding false origin transitions in the SVLF spectra, the S_0 frequencies are determined to 420 and 533 cm^{-1}, which is in quite good agreement with the calculated results of 401 and 535 cm^{-1}.

The emission spectra out of the two levels 780 and 938 cm^{-1} above the S_1 origin consist of partially resolvable sharp emission features on a broader background, as seen in Figure 9 and Figure 10. Although vibrational state mixing leads to the appearance of congested false origin spectra at even lower energy, the 780 cm^{-1} level in S_1 is the lowest energetic level in the first excited electronic state showing an almost unresolvable spectrum. The assignment of this spectrum is therefore quite difficult. We tentatively assign it to originate from the overtone excitation of the out-of-plane mode ν_{54}. First, the excitation band is quite weak, as many observed out-of-plane overtone bands. Second, the observed spectrum indicates a large frequency shift between S_0 and S_1, typically observed for several out-of-plane modes. Thirdly, calculated frequencies of mode ν_{54} (see Table 2) indicate a large frequency shift between the two electronic states, and the calculated values fit well to the observed frequencies. Note that the strongest, sharp emission feature in the false origin region occurs at 934 cm^{-1}. Assuming that this band is the true false origin, a ground state frequency of 467 cm^{-1} is obtained.

The excited-state level at 938 cm^{-1}, which also shows a strongly congested false origin region (see Figure 10), contains some overtone character of mode ν_{38} due to the appearance of a strong 38_1^2 band at 508 cm^{-1}. Assuming harmonic frequencies, the S_1 level 38^2 is expected to lie at 940 cm^{-1}, only 2 cm^{-1} higher than observed. The difference could certainly be due to anharmonicity. As seen from Figure 4, the excitation level at 938 cm^{-1} is the strongest band within a congested group of levels, most of them assignable to overtone transitions of the corresponding levels in the spectral range of 460 to 470 cm^{-1}, where strong vibrational state mixing was observed. It is

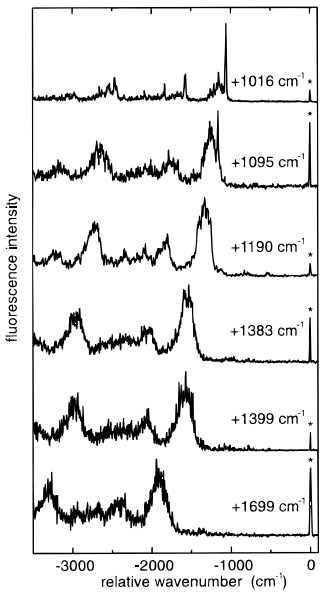

Figure 11. Dispersed SVLF spectra obtained following excitation of bands above 1000 cm^{-1} vibrational energy in S_1 of *cis*-2MXN. Transitions are measured relative to the excitation position which is indicated by an asterisk in each case.

therefore not surprising that the SVLF spectrum out of level 38^2 shows an increased congestion.

5.2.5. Modes with Energy $E_{vib}(S_1)$ > 1000 cm^{-1}. Figure 11 shows several emission spectra obtained from vibronic levels with vibrational energies of more than 1000 cm^{-1} in the S_1 state of *cis*-2MXN. Relaxed emission now becomes the dominant part of the SVLF spectra in this excitation energy range. Only the SVLF spectra of the two vibronic excitation frequencies at 1016 cm^{-1} and 1095 cm^{-1} still exhibit sharp false origin transitions distinguishable from the relaxed background, revealing that two fundamental ground state vibrations with frequencies of 1050 cm^{-1} (possibly ν_{29}) and 1156 cm^{-1} (possibly ν_{27}) may be involved, although these assignments remain speculative. The SVLF spectrum out of the 1016 cm^{-1} band shows additional sharp bands at 1061, 1143, and 1201 cm^{-1}. The 1201 cm^{-1} band could belong to the $39_1^0\,34_1^0$ transition, also observed in the origin excited SVLF spectrum. No assignment could be made in the case of the other two emission bands.

In the case of the four vibronic bands 1190, 1399, 1434, and 1699 cm^{-1} above the origin S_1 level, we were no longer able to extract the ground state vibrational frequencies due to the lack of any structured emission in their dispersed emission spectra. Dissipative IVR seems to occur, preventing the appearance of any sharp, unrelaxed emission out of the initially excited state. This is in agreement with our previous finding of restricted IVR in the time and frequency resolved emission of the vibronic band 978 cm^{-1} above the vibrationless S_1 level.[15]

6. Discussion

In this report we presented SVLF spectra from 25 vibronic levels of *cis*-2MXN accessible via the $S_1 \leftarrow S_0$ transition. Our assignments of the various SVLF spectra were guided by the results of ab initio calculations, and in the following we further discuss our proposed assignments for both electronic states. Furthermore, we also elaborate several aspects of vibrational interaction which could be responsible for the observed pattern of vibrational state mixing in various SVLF spectra.

6.1. Vibrational assignments of S_1 Frequencies. Calculated normal-mode frequencies are summarized in Table 4 in comparison with experimentally determined frequencies of low energy modes (<1000 cm^{-1}). They are numbered in order of decreasing S_0 frequency in each irreducible representation. Because of the apparent broadening in the SVLF spectra of S_1 levels above 1000 cm^{-1} of vibrational energy, which made further assignments either very speculative or even impossible, only vibrations below this energy are discussed here. In general, all vibronic transitions $A' \leftrightarrow A'$ and $A'' \leftrightarrow A'$ are electric dipole allowed in the C_s symmetry group, although excitations involving A'' levels would only occur from the vibrationless ground state if the transition dipole moment would contain a component lying in the out-of-plane direction of *cis*-2MXN, perpendicular to the aromatic plane. On the other hand, CIS calculations showed that the $S_1 \leftarrow S_0$ is a $\pi-\pi^*$ transition which exhibits an in-plane transition dipole moment. Therefore, vibronic transitions involving out-of-plane modes a″ should occur only as overtone bands obeying the vibrational selection rule $\Delta v = 2$.

TABLE 4: Comparison between Experimental and Theoretical Vibrational Frequencies of In-plane (a′) and out-of-plane (a″) Modes up to 1000 cm^{-1} in the Ground State S_0 and in the First Excited State S_1 of *cis*-2MXN[a]

symmetry	mode	S_0 exptl (cm^{-1})	S_0 calcd (cm^{-1})	S_1 exptl (cm^{-1})	S_1 calcd (cm^{-1})
a′	31	1019	992	978	993
	32	954	937	915	908
	33	900	884	n/a	865
	34	772	756	722	718
	35	701	683	667	665
	36	623	611	n/a	582
	37	523	509	476	500
	38	508	495	470	472
	39	432	421	n/a	397
	40	n/a	333	n/a	329
	41	196	189	192	190
a″	45	n/a	991	n/a	875
	46	n/a	975	n/a	864
	47	n/a	885	n/a	816
	48	n/a	859	n/a	797
	49	n/a	827	n/a	736
	50	n/a	760	n/a	672
	51	n/a	756	n/a	700
	52	n/a	647	n/a	584
	53	533	535	434	481
	54	467	478	390	390
	55	420	401	348	335
	56	311	313	256	266
	57	232	237	202	214
	58	182	183	139	151
	59	106	129	100	115
	60	80	72	70	55

[a] Calculated frequencies are scaled by 0.9.

Out of the 27 vibrations (16 out-of-plane and 11 in-plane modes) listed in Table 4, 15 experimentally determined S_1 frequencies could be correlated to the (scaled) normal mode frequencies of the CIS calculations. The average deviation between the calculated and the experimental frequencies is ±11 cm^{-1}. The largest relative deviations were obtained for the two lowest energetic out-of-plane modes ν_{60} (−21%) and ν_{59} (+15%). In general, the in-plane modes show a better agreement between theory and experiment. The proposed assignments in the case of the two modes ν_{54} and ν_{53} are only tentative, all other assignments have a quite high degree of certainty due to multiple assignments in various SVLF spectra.

As seen from Table 4, we could assign in-plane modes up to 1000 cm^{-1} in energy in S_1, but no out-of-plane mode could be assigned with an energy higher than 500 cm^{-1}. Although this might be due to small FC factors in the case of the out-of-

plane modes, mode selective IVR might also explain this fact. The onset of strong vibrational coupling in S_1 is seen in the SVLF spectra at 780 cm^{-1} above the S_1 origin. This band was assigned to an out-of-plane overtone excitation of ν_{54}. On the other hand, in-plane mode excitations even higher in energy, like 32_0^1 at 915 cm^{-1} and 31_0^1 at 978 cm^{-1}, still exhibit resolvable SVLF spectra, although some restricted IVR is present.[15] One reason for stronger mixing of the out-of-plane modes, and therefore a lower onset of dissipative IVR, might be larger frequency differences of the out-of-plane vibrations between the two electronic states. Typically, out-of-plane frequencies change on the order of 5−15%, whereas in-plane frequency differences are only 2−5%. This leads to the appearance of larger coeffients in the Duschinsky matrix of the out-of-plane modes (*i.e.*, indicating a greater state mixing). Furthermore, the three lowest energetic modes in S_1 are out-of-plane vibrations, having two to three times lower frequencies than the lowest energetic in-plane mode in S_1. This leads to an increased state density of out-of-plane modes compared to in-plane vibrations at the same amount of internal energy, which might favor dissipative IVR. Although our results lack any quantitative measurement of IVR so far, they seem to be in agreement with similar experiments performed by Smalley and co-workers on phenoxyalkanes and alkylbenzenes.[32] In the case of the phenoxyalkanes, dispersed emission studies seemed to show evidence for facile vibrational relaxation due to the presence of anharmonic chain torsions and bends, although this interpretation was questioned on the ground of spectral simulations performed by Brumer and co-workers.[33]

All S_1 levels assigned in our study of the $S_1 \leftarrow S_0$ obey the selection rules for a C_s symmetry group. So far no out-of-plane mode could be found exhibiting a $\Delta v = 1$ transition. This is in agreement with a planar structure of *cis*-2MXN in S_1 ($^1A'$ state), as obtained in our CIS calculations. If a nonplanar structure would be present in the S_1 electronic state, large progressions of several out-of-plane modes would have to appear due to their considerable frequency changes, which was not observed.

6.2. Vibrational Assignments of S_0 Frequencies. The experimentally determined ground state vibrational frequencies are also listed in Table 4 in comparison with the results of the ab initio calculations. Again, only modes up to 1000 cm^{-1} are given.

In the case of the 11 in-plane modes below 1000 cm^{-1} in S_0, 10 experimental frequencies could be observed and assigned to originate from in-plane vibrations as seen in Table 4. Using a scaling factor of 0.9 for the calculated mode frequencies, the average difference between the calculated and observed in-plane frequencies of the 10 assigned modes is 15 cm^{-1}. Since all in-plane mode frequencies are calculated too low if this scaling factor is used, a slight adjustment of the scaling factor to 0.92 increases the agreement between observed and calculated frequencies to ± 3 cm^{-1}, which indicates a quite good agreement. Aside from mode ν_{39}, whose assignment is only tentative due to the lack of sufficient transitions observed, all other in-plane mode assignments are fairly trustworthy. No evidence could yet be found for the in-plane mode ν_{40}, calculated at 333 cm^{-1} in S_0. Its FC factor might be very small, because the ab initio calculations predicted a negligible frequency change between S_0 and S_1, as well as a very small displacement vector ΔQ (see Table 2).

Eight low-frequency out-of-plane modes in the electronic ground state of *cis*-2MXN could also be assigned to calculated frequencies through the analyses of the various SVLF spectra. These assignments are also included in Table 4. Thereby, the four modes ν_{60} to ν_{57} are highly active in the low energy part of the FEX spectrum and origin excited SVLF spectrum. All of them appear as $\Delta v = 2$ overtone transitions in both spectra. The two modes ν_{60} and ν_{58} also appear in a combination band in the FEX ($60_0^1 58_0^1$) and in the 0_0^0 SVLF spectrum ($60_1^0 58_1^0$), although these transitions would be strictly forbidden in the harmonic zero order approximation (see discussion below). Mode ν_{57} also seems to play an important role in the vibrational state mixing of levels approximately 460 cm^{-1} above the vibrationless S_1 origin. Together with mode ν_{60}, mode ν_{57} is involved in various combination bands in this energy range, often in combination with the in-plane mode ν_{41}. This is understood due to the fact that ν_{60} corresponds to the methoxy torsion, ν_{57} to the methyl torsion, and ν_{41} to the in-plane methoxy bending vibration. In order to reduce steric interaction between close lying methoxy group and naphthalene group hydrogen atoms, higher excitations of the methoxy torsion are coupled to the methyl torsion and methoxy bending motion. As seen from Table 4, the calculated ab initio frequencies of modes ν_{60} to ν_{57} agree quite well with the experimental values. The calculations correctly predicted large frequency changes on the order of 10−15% for all four modes between S_0 and S_1. Therefore, the overtone transitions become apparent in the FEX spectrum, in agreement with experiment.

The assignments of the four out-of-plane modes ν_{56} to ν_{53} are less confident because of the reduced amount of experimental evidence. Most questionable is the assignment of mode ν_{54}, which shows the lowest energetic SVLF spectrum with extensive, unresolvable emission features. These excitation transitions are of similar low intensities in the FEX spectrum as the overtone bands observed in the case of ν_{60} to ν_{57}. No predicted in-plane mode frequency could fit well to these experimental frequencies in both electronic states, whereas the calculated out-of-plane frequencies correspond well to the observed values. The average frequency difference between the calculated and experimentally observed frequencies is ± 8 cm^{-1} (using a scaling factor of 0.9), which is quite satisfactory. Therefore, our assignments of these modes seem to be supported by our ab initio calculations.

6.3. Duschinsky Rotation and Vibronic Coupling. As shown in sections 5.2.3 and 5.2.4, several SVLF spectra of *cis*-2MXN reveal extensive mode mixing through the appearance of crossed sequence transitions in the false origin region, even at low vibrational excess energy in S_1. These crossed sequence transitions of the form $X_0^n Y_n^0$ in the SVLF spectra of an optically active mode X indicate the presence of substantial mode mixing through Duschinsky rotation, otherwise only transitions out of the optically excited mode X would be observed.[34−36] Thereby, only modes which belong to the same irreducible representation within a given symmetry group of the molecule can be mixed by Duschinsky rotation. This means that in the case of a planar molecule like *cis*-2MXN, in-plane (a′) and out-of-plane (a″) modes remain strictly separated. This was confirmed in the present case of *cis*-2MXN using the calculated normal mode vectors. Analysis of the Duschinsky matrix showed that low energy modes (below 1000 cm^{-1}) are typically mixed with 1 or 2 neighboring modes of the same irreducible species, and mixing coefficients are on the order of 0.2−0.3. Analysis of the congested spectra shown in Figure 8 also indicated that in-plane levels are coupled to out-of-plane combination levels, which have the same overall vibrational symmetry a′. This coupling may be induced by accidental Fermi resonances. Our analysis given in section 5.2.3 suggests that

such a coupling mechanism is present in order to account for the extensive vibrational level mixing in the region 460 cm^{-1} above the vibrationless S_1 level.

Further signatures for the occurrence of Duschinsky rotation in the S_1-S_0 spectra of *cis*-2MXN are various out-of-plane combination bands. The most prominent transition is the $60_0^1\,58_0^1$ in the FEX spectrum and the $60_1^0\,58_1^0$ band in the origin excited emission spectrum, but also observed are $60_1^2\,58_1^0$, $60_2^1\,58_0^1$, and $60_3^2\,58_0^1$ in the SVLF spectrum of the $60_0^1\,58_0^1$ band. These transitions cannot derive their intensities through a purely FC mechanism in the harmonic approximation, although their overall vibrational symmetry is a′. Similar combination bands of nontotally symmetric vibrations were found in the excitation and emission spectra of benzene,[37] *m-/p*-difluorobenzene,[38,39] and several substituted styrenes.[40] The appearance was accounted for as being either due to the Duschinsky effect, which weakens the selection rules for nontotally symmetric vibrations or due to second-order HT coupling with a higher excited state. Our analysis of various SVLF spectra of *cis*-2MXN indicates that the Duschinsky effect is highly active. Transitions with a formal assignment $X_0^1\,Y_0^1$ in excitation (or $X_1^0\,Y_1^0$ in emission) of two out-of-plane modes X and Y may gain their intensity due to the Duschinsky induced introduction of X_0^2 and Y_0^2 (or X_2^0 and Y_2^0) character in the total transition moment. We will further investigate the appearance of these out-of-plane combination bands in various spectra of *cis*-2MXN through spectral simulations of FC intensities employing the calculated Duschinsky matrix.

Similar experimental results of vibrational state mixing in S_1 due to Duschinsky rotation were found recently in studies of the vibronic spectroscopy of 2-methylnaphthalene (2MN)[2,3] and *trans*-1-hydroxynaphthalene (*trans*-1HN).[9,10] In both cases the spectral region around the parental naphthalene mode ν_8 is involved. This is the same energy region in S_1 where extensive state mixing was found in the SVLF spectra of *cis*-2MXN, although the assignment of the parental naphthalene mode ν_8 is not unambiguous in this case. For 2MN and *trans*-1HN, vibronic coupling with the second electronic state (^1L_a) is proposed as the cause of rotation. This is supported by absorption/emission mirror asymmetry and some evidence found in the rotationally resolved spectrum of the 414 cm^{-1} S_1 band of *trans*-1HN.[9]

Compared to 2MN and *trans*-1HN, excited state calculations of *cis*-2MXN revealed a state reversal of the first two excited electronic states compared with naphthalene. Whereas S_1 of 2MN and *trans*-1HN are correlated with ^1L_b of parental naphthalene, and S_2 with ^1L_a, the reverse state ordering is predicted by our CIS calculations in the case of *cis*-2MXN. A similar situation was also found for 1-aminonaphthalene (1AN), where a $^1L_b/^1L_a$ state reversal was established by rotationally resolved spectroscopy.[12] In spite of this reversed state ordering vibronically induced Duschinsky rotation remains possible if vibronic coupling is present between the two electronic states. This connection between Duschinsky rotation and vibronic coupling was nicely discussed by Small and co-workers,[36] indicating that a Duschinsky rotation is a consequence of two or more vibrations that borrow intensity from higher excited states. Either of the coupled states can be a source or a sink of Herzberg−Teller intensity for the other state, depending on the sign of the induced transition moment. To further investigate the case of *cis*-2MXN, it would be very instructive to obtain the rotationally resolved spectra for the various vibronic transitions approximately 460 cm^{-1} above the origin S_1 level.

7. Conclusions

The vibronic spectroscopy of the $S_1 \leftrightarrow S_0$ transition of *cis*-2MXN has been studied in a supersonic jet expansion. First vibrational assignments of observed frequencies in S_0 and S_1 are given on the basis of ab initio calculations. The molecule is calculated to be planar in both electronic states, allowing a spectral analysis assuming C_s symmetry. Furthermore, the conformation of 2MXN with the methoxy group in the *cis* configuration is calculated to be more stable (≈700 cm^{-1}) than the *trans* configuration in the ground electronic state. This is in agreement with a previous assignment of the fluorescence excitation spectrum of 2MXN.

The calculated normal-mode frequencies in S_0 and S_1 of *cis*-2MXN were compared with experimental frequencies obtained from the fluorescence excitation spectrum and various single vibronic level fluorescence spectra. Good agreement was found for modes in the energy range below 1000 cm^{-1} in both electronic states. Our analysis also indicated that several out-of-plane modes are highly active in the vibronic S_1-S_0 spectrum of *cis*-2MXN due to the large frequency changes between the two electronic states. The assignment of vibrational frequencies above 1000 cm^{-1} was confined by the onset of extensive congestion in the SVLF spectra.

Several SVLF spectra revealed clear signatures of strong vibrational state mixing in the excited state even at low internal energy. SVLF spectra obtained out of S_1 levels with less than 500 cm^{-1} vibrational energy showed multiple false origin transitions instead of a single $\Delta v = 0$ band. Most likely Duschinsky rotation of excited state normal modes is responsible for the appearance of vibrational state mixing, in addition to accidental Fermi resonances between fundamental in-plane levels and out-of-plane combination levels. The situation in *cis*-2MXN seems to be similar to vibrational state mixing observed in the SVLF spectra of 2-methylnaphthalene and *trans*-1-hydroxynaphthalene.

Detailed investigations are under way to simulate numerically the experimental SVLF spectra of *cis*-2MXN using calculated and experimental frequencies and normal mode displacements. CASSCF calculations will be performed to test the predicted $^1L_b/^1L_a$ state reversal in the CIS calculations. Furthermore, the vibronic S_1-S_0 spectroscopy of *cis*-2MXN will be compared with recently obtained spectra of *trans*-1-methoxynaphthalene in a forth-coming publication.

Acknowledgment. I thank Prof. S. Leutwyler for his interest in this work and the many facilities he provided and S. Graf for the help with the ab initio calculations. Financial support by the Schweizerische Nationalfonds (Grants 21-42185.94 and 21-45539.95) is gratefully acknowledged.

References and Notes

(1) Oikawa, A.; Abe, H.; Mikami, N.; Ito, M. *J. Phys. Chem.* **1984**, *88*, 5180.

(2) Warren, J. A.; Hayes, J. M.; Small, G. J. *J. Chem. Phys.* **1984**, *80*, 1786.

(3) Warren, J. A.; Hayes, J. M.; Small, G. J. *Chem. Phys.* **1986**, *102*, 313.

(4) Jacobson, B. A.; Guest, J. A.; Novak, F. A.; Rice, S. A. *J. Chem. Phys.* **1987**, *87*, 269.

(5) Lakshminarayan, C.; Knee, J. L. *J. Phys. Chem.* **1990**, *94*, 2637.

(6) Johnson, J. R.; Jordan, K. D.; Plusquellic, D. F.; Pratt, D. W. *J. Chem. Phys.* **1990**, *93*, 2258.

(7) Lahmani, F.; Bréhéret, E.; Zehnacker-Rentien, A.; Ebata, T. *J. Chem. Soc., Faraday Trans.* **1993**, *89*, 623.

(8) Pfanstiel, J. F.; Pratt, D. W. *J. Phys. Chem.* **1995**, *99*, 7258.

(9) Humphrey, S. J.; Pratt, D. W. *Chem. Phys. Lett.* **1996**, *257*, 169.

(10) Knochenmuss, R.; Muiño, P. L.; Wickleder, C. *J. Phys. Chem.* **1996**, *100*, 11218.
(11) Lahmani, F.; Zehnacker, A.; Denisov, G.; Furin, G. G. *J. Phys. Chem.* **1996**, *100*, 8633.
(12) Berden, G.; Meerts, W. L.; Plusquellic, D. F.; Fujita, I.; Pratt, D. W. *J. Chem. Phys.* **1996**, *104*, 3935.
(13) Knochenmuss, R.; Leutwyler S. *J. Chem. Phys.* 1989, *91*, 1268. Knochenmuss, R.; Smith, D. E. *J. Chem. Phys.* **1994**, *101*, 7327.
(14) Breen, J. J.; Peng, L. W.; Willberg, D. M.; Heikal, A.; Cong, P.; Zewail, A. H. *J. Chem. Phys.* **1990**, *92*, 805. Kim, S. K.; Breen, J. J.; Willberg, D. M.; Peng, L. W.; Heikal, A.; Syage, J. A.; Zewail, A. H. *J. Phys. Chem.* **1995**, *99*, 7421.
(15) Troxler, T.; Pryor, B. A.; Topp, M. R. *Chem. Phys. Lett.* **1997**, *274*, 71.
(16) Breen, P. J.; Bernstein, E. R.; Secor, H. V.; Seeman, J. I. *J. Am. Chem. Soc.* **1989**, *111*, 1958.
(17) Owen, N. L.; Hester, R. E. *Spectrochim. Acta* **1969**, *25A*, 343.
(18) Spellmeyer, D. C.; Grootenhuis, P. D. J.; Miller, M. D.; Kuyper, L. F.; Kollman, P. A. *J. Phys. Chem.* **1990**, *94*, 4483.
(19) Vincent, M. A.; Hillier, I. H. *Chem. Phys.* **1990**, *140*, 35.
(20) Siewert, S. S.; Spangler, L. H. *J. Phys. Chem.* **1995**, *99*, 9316.
(21) Troxler, T.; Topp, M. R.; Metzger, B. S.; Spangler, L. H. *Chem. Phys. Lett.* **1995**, *238*, 313.
(22) Wittmeyer, S. A.; Topp, M. R. *Chem. Phys. Lett.* **1989**, *163*, 261.
(23) Frisch, M. J.; Trucks, G. W.; Head-Gordon, M.; Gill, P. M. W.; Wong, M. W.; Foresman, J. B.; Johnson, B. G.; Schlegel, H. B.; Robb, M. A.; Replogle, E. S.; Gomperts, R.; Andres, J. L.; Raghavachari, K.; Binkley, J. S.; Gonzalez, C.; Martin, R. L.; Fox, D. J.; Defrees, D. J.; Baker, J.; Stewart, J. J. P.; Pople, J. A. GAUSSIAN 92, Revision B; Gaussian, Inc.: Pittsburgh, PA, 1992. Frisch, M. J.; Trucks, G. W.; Schlegel, H. B.; Gill, P. M. W.; Johnson, B. G.; Robb, M. A.; Cheeseman, J. R.; Keith, T.; Petersson, G. A.; Montgomery, J. A.; Raghavachari, K.; Al-Laham, M. A.; Zakrzewski, V. G.; Ortiz, J. V.; Foresman, J. B.; Cioslowski, J.; Stefanov, B. B.; Nanayakkara, A.; Challacombe, M.; Peng, C. Y.; Ayala, P. Y.; Chen, W.; Wong, M. W.; Andres, J. L.; Replogle, E. S.; Gomperts, R.; Martin, R. L.; Fox, D. J.; Binkley, J. S.; Defrees, D. J.; Baker, J.; Stewart, J. P.; Head-Gordon, M.; Gonzalez, C.; Pople, J. A. GAUSSIAN 94, Revision D. 4; Gaussian, Inc.: Pittsburgh, PA, 1995.
(24) Swiderek, P.; Hohlneicher, G.; Maluendes, S. A.; Dupuis, M. *J. Chem. Phys.* **1993**, *98*, 974.
(25) Negri, F.; Zgierski, M. *J. Chem. Phys.* **1996**, *104*, 3486.
(26) Jas, G. S.; Kuczera, K. *Chem. Phys.* **1997**, *214*, 229.
(27) Zilberg, S.; Haas, Y. *J. Chem. Phys.* **1995**, *103*, 20.
(28) Salman, R. A. *Spectrochim. Acta*, **1984**, *40A*, 229. Salman, R. A. *Magn. Reson. Chem.* **1985**, *23*, 119.
(29) *Handbook of Chemistry and Physics*, 70th ed.; CRC Press: Boca Raton, 1989.
(30) Beck, S. M.; Hopkins, J. B.; Powers, D. E.; Smalley, R. E. *J. Chem. Phys.* **1981**, *74*, 43.
(31) Gutmann, M.; Schönzart, P. F.; Hohlneicher, G. *Chem. Phys.* **1990**, *140*, 107.
(32) Hopkins, J. B.; Powers, D. E.; Smalley, R. E. *J. Chem. Phys.* **1981**, *74*, 6986. Hopkins, J. B.; Powers, D. E.; Smalley, R. E. *J. Chem. Phys.* **1980**, *73*, 683.
(33) Gruner, D.; Brumer, P. *J. Chem. Phys.* **1991**, *94*, 2848. Gruner, D.; Brumer, P. *J. Chem. Phys.* **1991**, *94*, 2862.
(34) Fischer, G. *Vibronic Coupling*; Academic Press: London, 1984.
(35) Duschinsky, F. *Acta Physicochim.* **1937**, *7*, 551.
(36) Craig, D. P.; Small, G. J. *J. Chem. Phys.* **1969**, *50*, 3827. Small, G. J. *J. Chem. Phys.* **1971**, *54*, 3300.
(37) Smith, W. L. *J. Mol. Spectrosc.* **1996**, *176*, 95.
(38) Knight, A. E. W.; Kable, S. H. *J. Chem. Phys.* **1988**, *89*, 7139.
(39) Graham, P. A.; Kable, S. H. *J. Chem. Phys.* **1995**, *103*, 6426.
(40) Hollas, J. M.; Taday, P. F. *J. Mol. Spectrosc.* **1992**, *153*, 587. Sinclair, W. E.; Yu, H.; Phillips, D.; Gordon, R. D.; Hollas, J. M.; Klee, S.; Mellau, G. *J. Phys. Chem.* **1995**, *99*, 4386.